SUPPLEMENTARY MATERIAL FOR:

A network of eIF2β interactions with eIF1 and Met-tRNA$_i$ promotes accurate start codon selection by the translation preinitiation complex

Anil Thakur, Laura Marler, and Alan G. Hinnebusch

Table S1. Plasmids used in this study.

Plasmid	Description	Parent Plasmid	Source or Reference
YCplac111	sc *LEU2* cloning vector		(1)
p1200	sc *URA3 SUI1* in YCp50		(2)
YCplac112	hc TRP cloning Vector		(1)
pJCB101	sc *LEU2 SUI1* in YCplac111		(3)
YEp24	hc *URA3* cloning vector		(4)
ATP114	sc *LEU2 sui1-Q31A* in YCplac111	pJCB101	This study
ATP115	sc *LEU2 sui1-Q31K* in YCplac111	pJCB101	This study
ATP116	sc *LEU2 sui1-Q31E* in YCplac111	pJCB101	This study
ATP117	sc *LEU2 sui1*-F108Ain YCplac111	pJCB101	This study
ATP118	sc *LEU2 sui1-F108D* in YCplac111	pJCB101	This study
ATP119	sc *LEU2 sui1-F108R* in YCplac111	pJCB101	This study
ATP124	sc *LEU2 sui1-Q31A-F108A* in YCplac111	pJCB101	This study
p367	sc *URA3 HIS4(ATG)-lacZ*		(5)
p391	sc *URA3 HIS4(TTG)-lacZ*		(5)
p180	sc *URA3 GCN4-lacZ* in YCp50		(6)
pPMB24	sc *URA3 SUI1-lacZ*		(3)
pPMB25	sc *URA3* $SUI1_{opt}$*-lacZ*		(3)
pC3502	sc *URA3* $^{-3}$AAA^{-1} el.uORF1 *GCN4-lacZ* in YCp50		(7)
pC4466	sc *URA3* $^{-3}$UAA^{-1} el.uORF1 *GCN4-lacZ* in YCp50		(7)
pC3503	sc *URA3* $^{-3}$UUU^{-1} el.uORF1 *GCN4-lacZ* in YCp50		(7)
pC3505	sc *URA3* el.uORF1-less *GCN4-lacZ* in YCp50		(7)
p1780-IMT	hc *URA3 SUI2, SUI3, GCD11, IMT4*	YEp24	(8)
p4385	hc *TRP1- SUI2, SUI3, GCD11, IMT4*	p1780-IMT	Christie Fekete
p4280/YCpSUI3-S264Y-W	sc *TRP1 SUI3-S264Y*	YCplac22	(9)
p4281/YCpTIF5-G31R-W	sc *TRP1 TIF5-G31R*	YCplac22	(9)
pTYB2-eIF1	*SUI1* in PTYB2	pTYB2	(10),(10)
pPMB97	*sui1-K60E* in pTYB2	pTYB2-eIF1	(11)
ATP172	*sui1-Q31E* in pTYB2	pTYB2-eIF1	This study
ATP173	*sui1-F108D* in pTYB2	pTYB2-eIF1	This study
ATP174	*sui1-F108R* in pTYB2	pTYB2-eIF1	This study
ATP175	*sui1-Q31A-F108A* in pTYB2	pTYB2-eIF1	This study
p921	*sc URA3 SUI3*	pRS316	(12)
p920	*sc LEU2 SUI3*	pRS315	Thomas Dever
LMP24	*sc LEU2 SUI3-E198A*	p920	This study
LMP27	*sc LEU2 SUI3-F217A*	p920	This study
LMP29	*sc LEU2 SUI3-F217A/Q221A*	p920	This study

Plasmid	Description	Parent Plasmid	Source or Reference
LMP32	*sc LEU2 SUI3-K170A*	p920	This study
LMP33	*sc LEU2 SUI3-K170A/S202A*	p920	This study
LMP37	*sc LEU2 SUI3-K214A*	p920	This study
LMP38	*sc LEU2 SUI3-S202A/K214A*	p920	This study
LMP94	*sc LEU2 SUI3-E189A*	p920	This study
LMP95	*sc LEU2 SUI3-E189R*	p920	This study
LMP96	*sc LEU2 SUI3-Q193A*	p920	This study
LMP97	*sc LEU2 SUI3-Q193R*	p920	This study
LMP98	*sc LEU2 SUI3-E189A/Q193A*	p920	This study
LMP99	*sc LEU2 SUI3-E189R/Q193R*	p920	This study
pAV1089	*hc URA3(6x)His-GCD11, SUI2, SUI3*	YEp24	(13)
pAV1726	*hc LEU2 (6x)His-GCD11, SUI2, SUI3*	pRS425	(14)
LMP91	*hc LEU2 (6x)His-GCD11, SUI2, SUI3-F217A/Q221A*	pAV1726	This study
LMP92	*hc LEU2 (6x)His-GCD11, SUI2, SUI3-S202A/K214A*	pAV1726	This study
LMP101	*hc LEU2 (6x)His-GCD11, SUI2, SUI3-E189R*	pAV1726	This study

Table S2. Yeast strains used in this study.

Strain	Genotype	Source
JCY03	*MATa ura3-52 leu2-3 leu2-112 trp1Δ-63 his4-301*(*ACG*) *sui1Δ::hisG* p1200 (sc *URA3 SUI1*)	(15)
ATY100 (PMY30)	*MATa ura3-52 leu2-3 leu2-112 trp1Δ-63 his4-301*(*ACG*) *sui1Δ::hisG* pJCB101 (sc *LEU2 SUI1*)	(3)
ATY122	*MATa ura3-52 leu2-3 leu2-112 trp1Δ-63 his4-301*(*ACG*) *sui1Δ::hisG* ATP114 (sc *LEU2 sui1-Q31A*)	This study
ATY123	*MATa ura3-52 leu2-3 leu2-112 trp1Δ-63 his4-301*(*ACG*) *sui1Δ::hisG* ATP115 (sc *LEU2 sui1-Q31K*)	This study
ATY124	*MATa ura3-52 leu2-3 leu2-112 trp1Δ-63 his4-301*(*ACG*) *sui1Δ::hisG* ATP116 (sc *LEU2 sui1Q31E*)	This study
ATY125	*MATa ura3-52 leu2-3 leu2-112 trp1Δ-63 his4-301*(*ACG*) *sui1Δ::hisG* ATP117 (sc *LEU2 sui1-F108A*)	This study
ATY126	*MATa ura3-52 leu2-3 leu2-112 trp1Δ-63 his4-301*(*ACG*) *sui1Δ::hisG* ATP118 (sc *LEU2 sui1-F108D*)	This study
ATY127	*MATa ura3-52 leu2-3 leu2-112 trp1Δ-63 his4-301*(*ACG*) *sui1Δ::hisG* ATP119 (sc *LEU2 sui1-F108R*)	This study
ATY128	*MATa ura3-52 leu2-3 leu2-112 trp1Δ-63 his4-301*(*ACG*) *sui1Δ::hisG* ATP124 (sc *LEU2 sui1-Q31A-F108A)*	This study
KAY18	*MATα leu2-3 leu2-112 ura3-53 ino1 sui3Δ gcn2Δ* p921(*SUI3, URA3*)	(8)
LMY103	*MATα leu2-3 leu2-112 ura3-53 ino1 sui3Δ gcn2Δ* LMP24(*SUI3-E198A, LEU2*)	This study
LMY106	*MATα leu2-3 leu2-112 ura3-53 ino1 sui3Δ gcn2Δ* LMP27(*SUI3-F217A, LEU2*)	This study
LMY108	*MATα leu2-3 leu2-112 ura3-53 ino1 sui3Δ gcn2Δ* LMP29(*SUI3-F217A/Q221A, LEU2*)	This study
LMY111	*MATα leu2-3 leu2-112 ura3-53 ino1 sui3Δ gcn2Δ* LMP32(*SUI3-K170A, LEU2*)	This study
LMY112	*MATα leu2-3 leu2-112 ura3-53 ino1 sui3Δ gcn2Δ* LMP33(*SUI3-K170A/S202A, LEU2*)	This study
LMY116	*MATα leu2-3 leu2-112 ura3-53 ino1 sui3Δ gcn2Δ* LMP37(*SUI3-K214A, LEU2*)	This study
LMY117	*MATα leu2-3 leu2-112 ura3-53 ino1 sui3Δ gcn2Δ* LMP38(*SUI3-S202A/K214A, LEU2*)	This study
LMY130	*MATα leu2-3 leu2-112 ura3-53 ino1 sui3Δ gcn2Δ* LMP94(*SUI3-E189A, LEU2*)	This study
LMY131	*MATα leu2-3 leu2-112 ura3-53 ino1 sui3Δ gcn2Δ* LMP95(*SUI3-E189R, LEU2*)	This study
LMY132	*MATα leu2-3 leu2-112 ura3-53 ino1 sui3Δ gcn2Δ* LMP96(*SUI3-Q193A, LEU2*)	This study
LMY133	*MATα leu2-3 leu2-112 ura3-53 ino1 sui3Δ gcn2Δ* LMP97(*SUI3-Q193R, LEU2*)	This study

Strain	Genotype	Source
LMY134	*MATα leu2-3 leu2-112 ura3-53 ino1 sui3Δ gcn2Δ* LMP98(*SUI3-E189A/Q193A, LEU2*)	This study
LMY135	*MATα leu2-3 leu2-112 ura3-53 ino1 sui3Δ gcn2Δ* LMP99(*SUI3-E189R/Q193R, LEU2*)	This study
LMY142	*MATα leu2-3 leu2-112 ura3-53 ino1 sui3Δ gcn2Δ* p920(*SUI3, LEU2*)	This study
H3840	*MATα leu2-3 leu2-112 ura3-52 ino1 sui2Δ gcn2Δ pep4::leu2::NatMX4 sui3::KANMX4 <HIS4-lacZ, ura3-52>* pAV1089(*SUI2, SUI3, [6x]-GCD11, URA3)*	(16)
LMY128	*MATα leu2-3 leu2-112 ura3-52 ino1 sui2Δ gcn2Δ pep4::leu2::NatMX4 sui3::KANMX4 <HIS4-lacZ, ura3-52>* LMP92(*SUI2, SUI3-S202A/K214A, [6x]-GCD11, URA3)*	This study
LMY129	*MATα leu2-3 leu2-112 ura3-52 ino1 sui2Δ gcn2Δ pep4::leu2::NatMX4 sui3::KANMX4 <HIS4-lacZ, ura3-52>* LMP91(*SUI2, SUI3-F217A/Q221A, [6x]-GCD11, URA3)*	This study
LMY137	*MATα leu2-3 leu2-112 ura3-52 ino1 sui2Δ gcn2Δ pep4::leu2::NatMX4 sui3::KANMX4 <HIS4-lacZ, ura3-52>* LMP101(*SUI2, SUI3-E189R, [6x]-GCD11, URA3)*	This study

Table S3. Oligonucleotide primers used in this study.

SUBSTITUTION	SEQUENCE 5' -3'
eIF1-Q31A FOR*	CTATATTCATATTCGTATCGCACAGAGAAATGGTAGAAAAACTTTAACTAC
eIF1-Q31A REV*	GTAGTTAAAGTTTTTCTACCATTTCTCTGTGCGATACGAATATGAATATAG
eIF1-Q31KFOR	CTATATTCATATTCGTATCAAACAGAGAAATGGTAGAAAAACTTTAACTACGG
eIF1-Q31K REV	CCGTAGTTAAAGTTTTTCTACCATTTCTCTGTTTGATACGAATATGAATATAG
eIF1-Q31E FOR	CAAACTATATTCATATTCGTATCGAACAGAGAAATGGTAGAAAAACTTTAAC
eIF1-Q31E REV	GTTAAAGTTTTTCTACCATTTCTCTGTTCGATACGAATATGAATATAGTTTG
eIF1-F108A FOR	GAAGAACATTAAAATTCATGGGGCTTAAGTTCAAGGCTTACGCCGAGTC
eIF1-F108A REV	GACTCGGCGTAAGCCTTGAACTTAAGCCCCATGAATTTTAATGTTCTTC
eIF1-F108D FOR	GAAGAACATTAAAATTCATGGGGATTAAGTTCAAGGCTTACGCCGAGTC
eIF1-F108D REV	GACTCGGCGTAAGCCTTGAACTTAATCCCCATGAATTTTAATGTTCTTC
eIF1-F108R FOR	GAAGAACATTAAAATTCATGGGCGTTAAGTTCAAGGCTTACGCCGAGTC
eIF1-F108R REV	GACTCGGCGTAAGCCTTGAACTTAACGCCCATGAATTTTAATGTTCTTC
eIF2β-E198A FOR	TTCAATATCTCTTCGCAGCATTAGGTACGTCCGGTTC
eIF2β-E198A REV	GAACCGGACGTACCTAATGCTGCGAAGAGATATTGAA
eIF2β-F217A FOR	GAAAAGATTAGTCATTAAGGGTAAGGCTCAATCCAAACAAATGGAGAATGTC
eIF2β-F217A REV	GACATTCTCCATTTGTTTGGATTGAGCCTTACCCTTAATGACTAATCTTTTC
eIF2β-F217A/Q221A FOR	GTCAGAAAAGATTAGTCATTAAGGGTAAGGCTCAATCCAAAGCAATGGAGAATGTCTTAAGAAGATACATTT
eIF2β-F217A/Q221A REV	AAATGTATCTTCTTAAGACATTCTCCATTGCTTTGGATTGAGCCTTACCCTTAATGACTAATCTTTTCTGAC

SUBSTITUTION	SEQUENCE 5’ -3’
eIF2β-K170A FOR	CTCCTGTTTGTTTGCGTGATGGTGCGAAGACTATTTTCTCGAATATCC
eIF2β-K170A REV	GGATATTCGAGAAAATAGTCTTCGCACCATCACGCAAACAAACAGGAG
eIF2β-S202A FOR	CGCAGAATTAGGTACGGCCGGTTCTGTTGACGG
eIF2β-S202A REV	CCGTCAACAGAACCGGCCGTACCTAATTCTGCG
eIF2β-K214A FOR	TTCTGTTGACGGTCAGAAAAGATTAGTCATTGCGGGTAAGTTTCAATCC
eIF2β-K214 REV	GGATTGAAACTTACCCGCAATGACTAATCTTTTCTGACCGTCAACAGAA
eIF2β-E189A FOR	CGAAAAATTGCATAGATCTCCGGCACATTTGATTCAATATCTCTTCG
eIF2β-E189A REV	CGAAGAGATATTGAATCAAATGTGCCGGAGATCTATGCAATTTTTCG
eIF2β-E189R FOR	GCCGAAAAATTGCATAGATCTCCGAGACATTTGATTCAATATCTCTTCGC
eIF2β-E189R REV	GCGAAGAGATATTGAATCAAATGTCTCGGAGATCTATGCAATTTTTCGGC
eIF2β-Q193A FOR	CATAGATCTCCGGAACATTTGATTGCATATCTCTTCGCAGAATTAGGTA
eIF2β-Q193A REV	TACCTAATTCTGCGAAGAGATATGCAATCAAATGTTCCGGAGATCTATG
eIF2β-Q193R FOR	GATCTCCGGAACATTTGATTCGATATCTCTTCGCAGAATTAGG
eIF2β-Q193R REV	CCTAATTCTGCGAAGAGATATCGAATCAAATGTTCCGGAGATC
eIF2β-E189A/Q193A FOR	CGAAAAATTGCATAGATCTCCGGCACATTTGATTGCATATCTCTTCGCAGAATTAGGTA

SUBSTITUTION	SEQUENCE 5’ -3’
eIF2β-E189A/Q193A REV	TACCTAATTCTGCGAAGAGATATGCAATCAAATGTGCCGGAGATCTATGCAATTTTTCG
eIF2β-E189R/Q193R FOR	CGAAAAATTGCATAGATCTCCGAGACATTTGATTCGATATCTCTTCGCAGAATTAGGTA
eIF2β-E189R/Q193R REV	TACCTAATTCTGCGAAGAGATATCGAATCAAATGTCTCGGAGATCTATGCAATTTTTCG

*FOR, forward primer ; REV, reverse primer

REFERENCES FOR SUPPLEMENTAL MATERIAL

1. Gietz RD & Sugino A (1988) New yeast-Escherichia coli shuttle vectors constructed with in vitro mutagenized yeast genes lacking six-base pair restriction sites. *Gene* 74(2):527-534.
2. Yoon HJ & Donahue TF (1992) The suil suppressor locus in Saccharomyces cerevisiae encodes a translation factor that functions during tRNA(iMet) recognition of the start codon. *Mol Cell Biol* 12(1):248-260.
3. Martin-Marcos P, Cheung YN, & Hinnebusch AG (2011) Functional elements in initiation factors 1, 1A, and 2beta discriminate against poor AUG context and non-AUG start codons. *Mol Cell Biol* 31(23):4814-4831.
4. Parent SA, Fenimore CM, & Bostian KA (1985) Vector systems for the expression, analysis and cloning of DNA sequences in S. cerevisiae. *Yeast* 1(2):83-138.
5. Donahue TF & Cigan AM (1988) Genetic selection for mutations that reduce or abolish ribosomal recognition of the HIS4 translational initiator region. *Mol Cell Biol* 8(7):2955-2963.
6. Hinnebusch AG (1985) A hierarchy of trans-acting factors modulates translation of an activator of amino acid biosynthetic genes in Saccharomyces cerevisiae. *Mol Cell Biol* 5(9):2349-2360.
7. Visweswaraiah J, Pittman Y, Dever TE, & Hinnebusch AG (2015) The beta-hairpin of 40S exit channel protein Rps5/uS7 promotes efficient and accurate translation initiation in vivo. *Elife* 4:e07939.
8. Asano K, Krishnamoorthy T, Phan L, Pavitt GD, & Hinnebusch AG (1999) Conserved bipartite motifs in yeast eIF5 and eIF2Bepsilon, GTPase-activating and GDP-GTP exchange factors in translation initiation, mediate binding to their common substrate eIF2. *EMBO J* 18(6):1673-1688.
9. Valasek L, Nielsen KH, Zhang F, Fekete CA, & Hinnebusch AG (2004) Interactions of eukaryotic translation initiation factor 3 (eIF3) subunit NIP1/c with eIF1 and eIF5 promote preinitiation complex assembly and regulate start codon selection. *Mol Cell Biol* 24(21):9437-9455.
10. Acker MG, Kolitz SE, Mitchell SF, Nanda JS, & Lorsch JR (2007) Reconstitution of yeast translation initiation. *Methods Enzymol* 430:111-145.
11. Martin-Marcos P, *et al.* (2013) beta-Hairpin loop of eukaryotic initiation factor 1 (eIF1) mediates 40 S ribosome binding to regulate initiator tRNA(Met) recruitment and accuracy of AUG selection in vivo. *J Biol Chem* 288(38):27546-27562.
12. Dever TE, Yang W, Astrom S, Bystrom AS, & Hinnebusch AG (1995) Modulation of tRNA(iMet), eIF-2, and eIF-2B expression shows that GCN4 translation is inversely coupled to the level of eIF-2.GTP.Met-tRNA(iMet) ternary complexes. *Mol Cell Biol* 15(11):6351-6363.
13. Pavitt GD, Ramaiah KV, Kimball SR, & Hinnebusch AG (1998) eIF2 independently binds two distinct eIF2B subcomplexes that catalyze and regulate guanine-nucleotide exchange. *Genes Dev* 12(4):514-526.
14. Gomez E, Mohammad SS, & Pavitt GD (2002) Characterization of the minimal catalytic domain within eIF2B: the guanine-nucleotide exchange factor for translation initiation. *EMBO J* 21(19):5292-5301.

15. Cheung YN, *et al.* (2007) Dissociation of eIF1 from the 40S ribosomal subunit is a key step in start codon selection in vivo. *Genes Dev* 21(10):1217-1230.
16. Martin-Marcos P, *et al.* (2014) Enhanced eIF1 binding to the 40S ribosome impedes conformational rearrangements of the preinitiation complex and elevates initiation accuracy. *RNA* 20(2):150-167.

Fig. S1

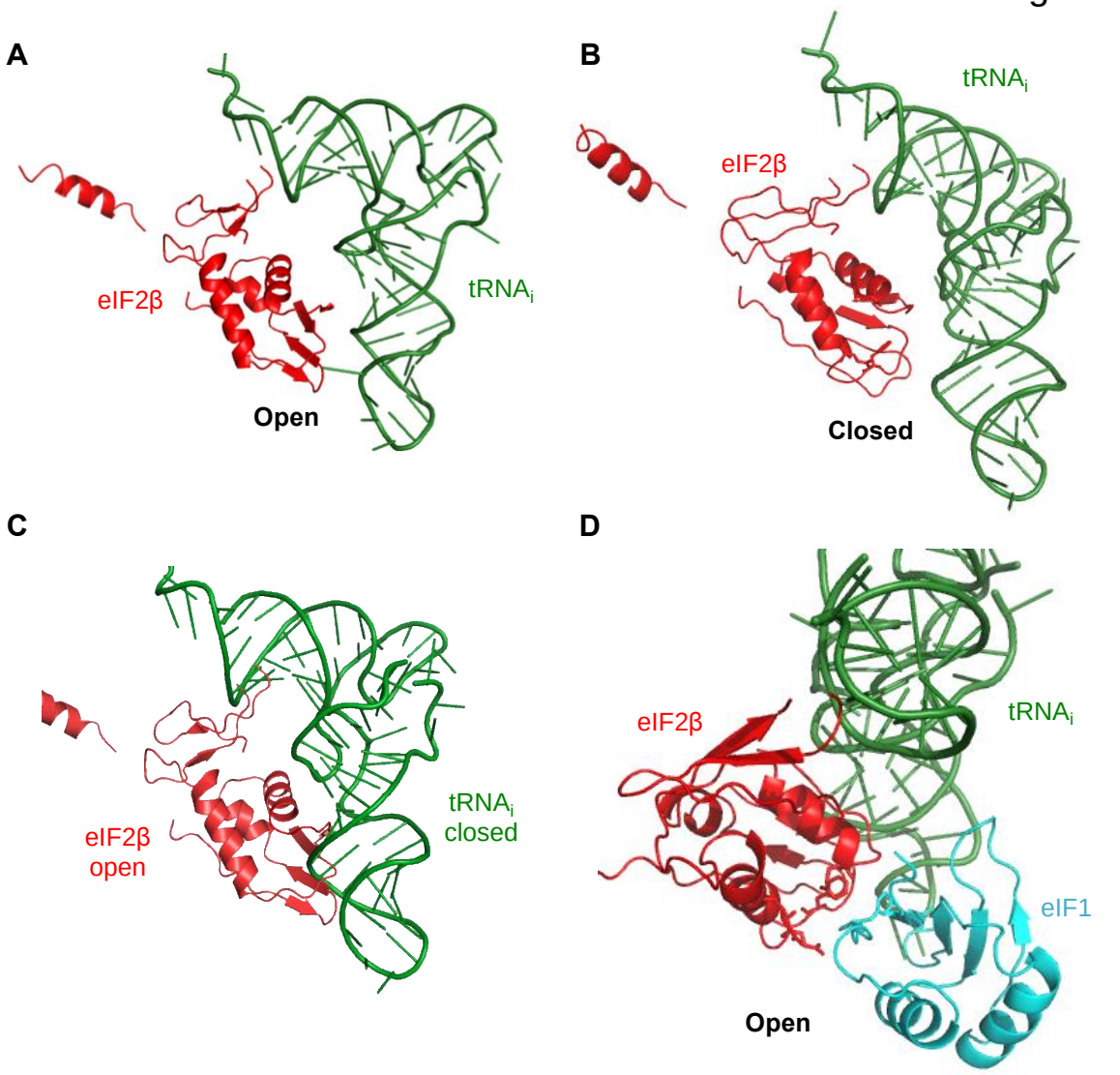

Fig. S1. Distinct interactions of eIF2β with $tRNA_i$ in py48S-open versus py48S-closed should enable eIF2β to restrict transition to the closed/P_{IN} conformation of the PIC in a manner facilitated by eIF1. (A) Interactions between eIF2β and the $tRNA_i$ ASL and D-loop in the py48S-open complex. **(B)** Interactions of eIF2β with $tRNA_i$ in py48S-closed differ from those in (A) and are restricted to the D-loop. **(C)** An overlay of eIF2β in py48S-open with $tRNA_i$ in py48S-closed reveals predicted clashes throughout the ASL. These clashes are alleviated during the open-to-closed transition by movement of eIF2β both laterally and toward the D-loop. The predicted clashes suggest that eIF2β performs a steric role in ensuring acccurate start codon selection, undergoing a conformational change that allows $tRNA_i$ to assume the P_{IN} state of the closed conformation only when a perfect AUG:anticodon duplex is formed in the P-site. **(D)** A network of interactions between eIF2β and both eIF1 and $tRNA_i$ in py48S-open enhances TC recruitment and stabilizes the open, scanning conformation of the PIC prior to AUG selection.

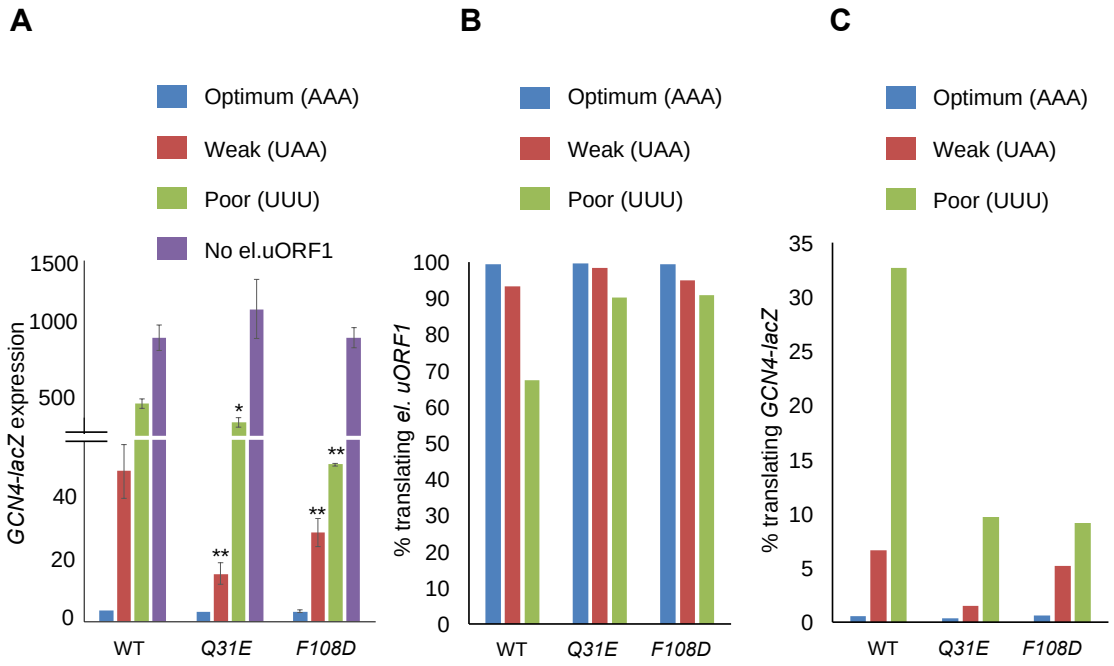

Fig. S2. eIF1 substitutions Q31E and F108D decrease discrimination against the *GCN4* uORF1 AUG codon in suboptimal context. (A) Transformants of JCY03 harboring WT *SUI1*, *sui1-Q31E* or *sui1-F108D* and el.uORF1 *GCN4-lacZ* reporters (pC3502, pC3503 or pC4466) containing, respectively, optimum, weak or poor context of uAUG-1, or an uORF-less *GCN4-lacZ* reporter with a mutated uAUG-1 (pC3505), were assayed for b-galactosidase activities as in Fig. 2D. Mean expression values with SEMs were determined from six transformants and asterisks indicate significant differences between mutant and WT as judged by a two-tailed, unpaired Student's t test (*P < 0.05; **P < 0.01). **(B, C)** The percentages of scanning ribosomes that translate el.uORF1 (B) or leaky-scan uAUG-1 and translate *GCN4-lacZ* (C) were calculated from the data in (A) by comparing the amount of *GCN4-lacZ* expression observed for each uORF-containing reporter to the uORF-less construct, yielding the percentages in (C), and subtracting the values in (C) from 100 to obtain the percentages in (B).

Fig. S3

A

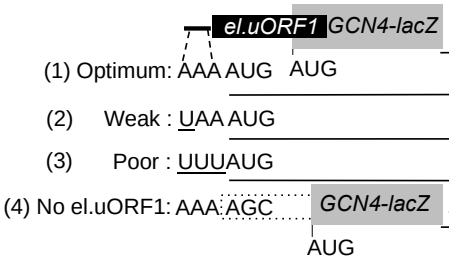

	GCN4-lacZ expression(U)			% translating *GCN4-lacZ*			% translating *el. uORF1*		
	(1) WT	(2) *Q31A*	(3) *F108A*	(4) WT	(5) *Q31A*	(6) *F108A*	(7) WT	(8) *Q31A*	(9) *F108A*
(1) Optimum: AAA AUG AUG	5±0.7	2±0.6**	3±0.2*	0.5	0.2	0.3	99.5	99.8	99.7
(2) Weak : UAA AUG	66±11	17±2**	8±5**	8	2	1	92	98	99
(3) Poor : UUUAUG	327±43	80±7**	158±15**	33	9	16	67	91	84
(4) No el.uORF1: AAA AGC GCN4-lacZ AUG	1000±150	900±200	1000±100	>99	>99	>99	<1	<1	<1

B

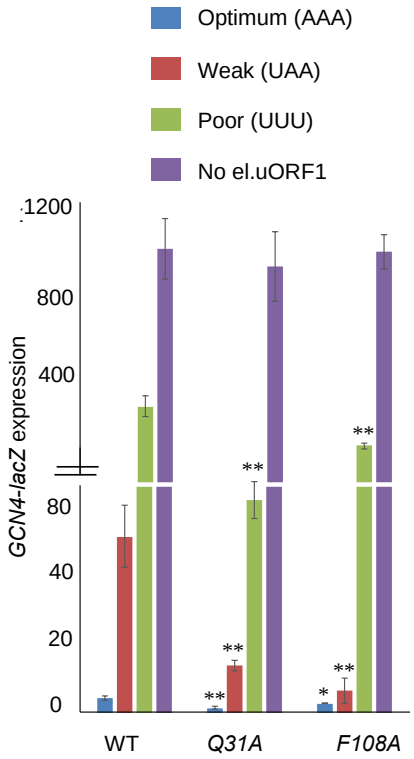

C

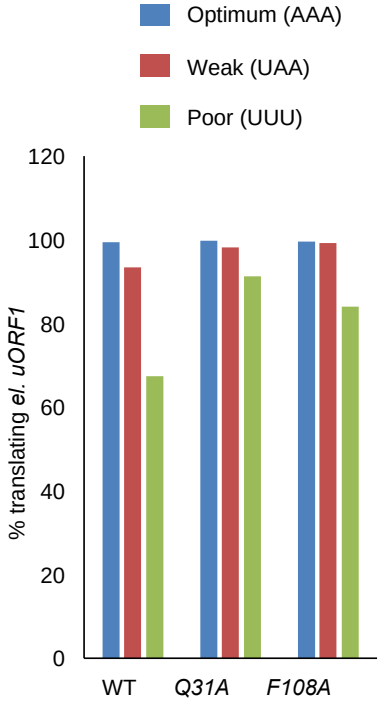

D

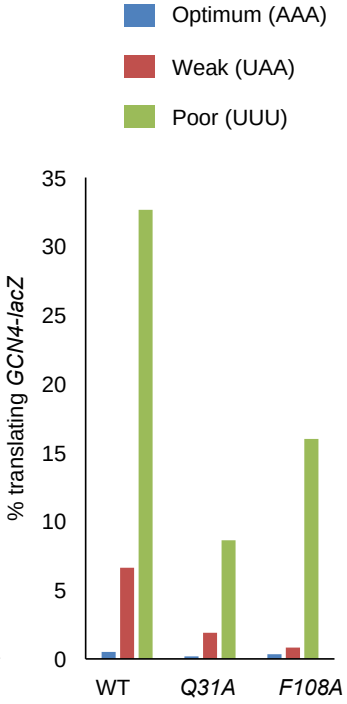

Fig. S3. eIF1 substitutions Q31A and F108A decrease discrimination against the *GCN4* uORF1 AUG codon in suboptimal context. (A) Transformants of JCY03 harboring WT *SUI1*, *sui1-Q31A* and *eIF1-F108A* and the el. uORF1 *GCN4-lacZ* reporters containing optimum (row 1), weak (row 2) or poor (row 3) context of uAUG-1, or an uORF-less *GCN4-lacZ* reporter with a mutated uAUG-1 (row 4), were analyzed as in Fig. 3C. **(B)** b-galactosidase activities from columns 1-3 of (A) plotted in graphical format for WT *SUI1*, *sui1*-Q31A or *sui1-F108A* transformants containing the el. uORF1 *GCN4-lacZ* reporters with optimum, weak or poor context of uAUG-1, or an uORF-less *GCN4-lacZ* reporter with a mutated uAUG. Mean expression values with SEMs were determined from six transformants and asterisks indicate significant differences between mutant and WT as judged by a two-tailed, unpaired Student's t test (*P < 0.05; **P <0.01). **(C, D)** The percentages of scanning ribosomes that translate el.uORF1 (C) or leaky-scan uAUG-1 and translate *GCN4-lacZ* (D) were calculated from the data in (B) as described in Fig. S2B-C.

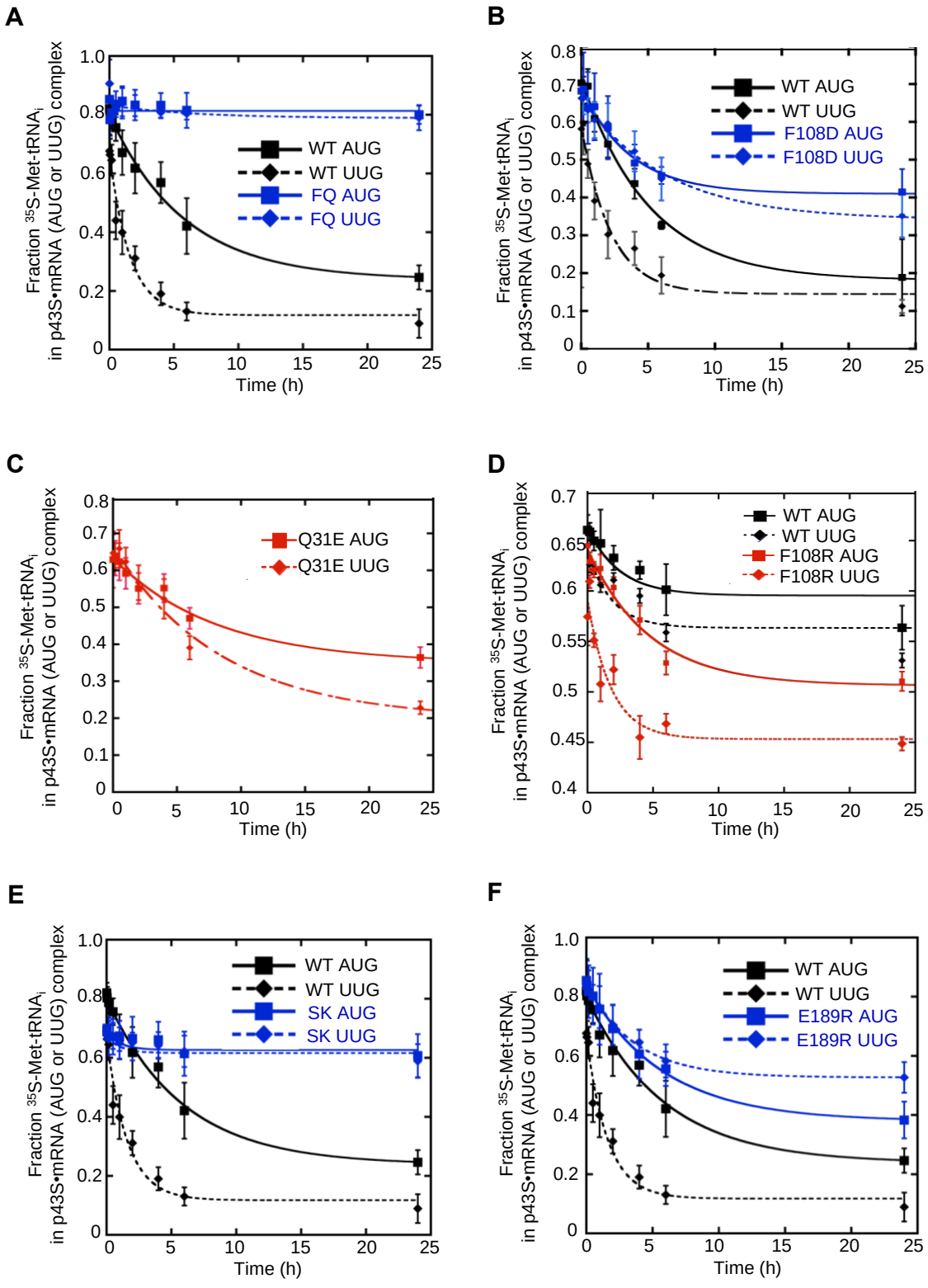
A
Fraction 35S-Met-tRNAi in p43S•mRNA (AUG or UUG) complex
Time (h)
WT AUG
WT UUG
FQ AUG
FQ UUG
B
Fraction 35S-Met-tRNAi in p43S•mRNA (AUG or UUG) complex
Time (h)
WT AUG
WT UUG
F108D AUG
F108D UUG
C
Fraction 35S-Met-tRNAi in p43S•mRNA (AUG or UUG) complex
Time (h)
Q31E AUG
Q31E UUG
D
Fraction 35S-Met-tRNAi in p43S•mRNA (AUG or UUG) complex
Time (h)
WT AUG
WT UUG
F108R AUG
F108R UUG
E
Fraction 35S-Met-tRNAi in p43S•mRNA (AUG or UUG) complex
Time (h)
WT AUG
WT UUG
SK AUG
SK UUG
F
Fraction 35S-Met-tRNAi in p43S•mRNA (AUG or UUG) complex
Time (h)
WT AUG
WT UUG
E189R AUG
E189R UUG

Fig. S4. Plots of TC dissociation assays with error. (A-E) To measure TC dissociation kinetics, as summarized schematically in Fig. 5D, partial 48S complexes were assembled with eIF1A, model mRNA containing an AUG or UUG start codon, radiolabeled TC containing either WT or mutant eIF2b, and either WT or mutant eIF1. Following incubation at 26° C for two hours, each reaction was chased with excess unlabeled TC for increasing periods of time and the fraction of labeled Met-tRNA$_i$ bound to the PIC at each time-point was determined via EMSA. Data from each gel were plotted individually to determine a dissociation rate (k_{off}). Representative plots are shown in Figs. 5E, 5H, 7C, 8G, and 9E. The rates from three independent experiments were averaged to determine the k_{off} values shown in Figs. 5F, 5I, 7D, 8H, and 9F. In order to give a visual representation of the variability across gels, we have averaged together values at each time point across three independent experiments and plotted an average curve with SEMs for eIF2b-F217A/Q221A (A), eIF1-F108D (B), eIF1-Q31E (C), eIF1-F108R (D), eIF2b-S202A/K214A (E), and eIF2b-E189R (F).

Fig. S5

A

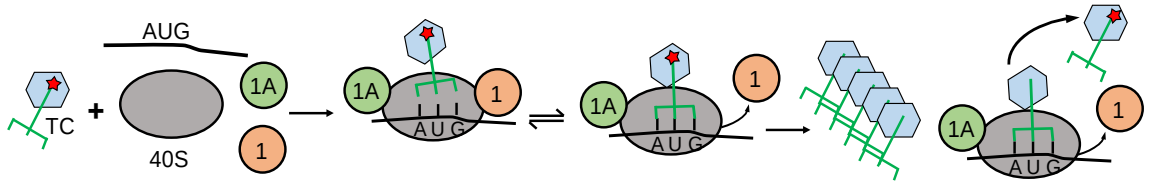
AUG
TC
+
40S
1A
1
1A
1
AUG
1A
1
AUG
1A
1
AUG

B

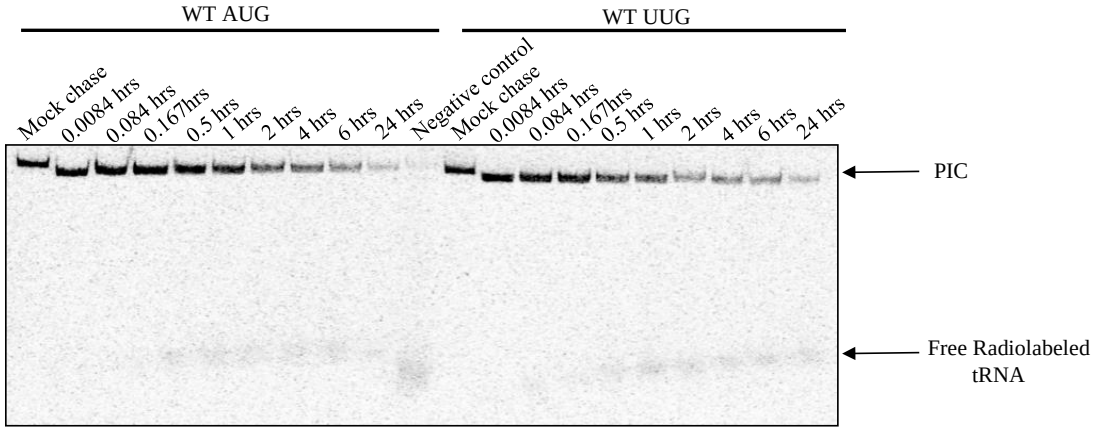
WT AUG
WT UUG
Mock chase
0.0084 hrs
0.084 hrs
0.167hrs
0.5 hrs
1 hrs
2 hrs
4 hrs
6 hrs
24 hrs
Negative control
Mock chase
0.0084 hrs
0.084 hrs
0.167hrs
0.5 hrs
1 hrs
2 hrs
4 hrs
6 hrs
24 hrs
PIC
Free Radiolabeled tRNA

C

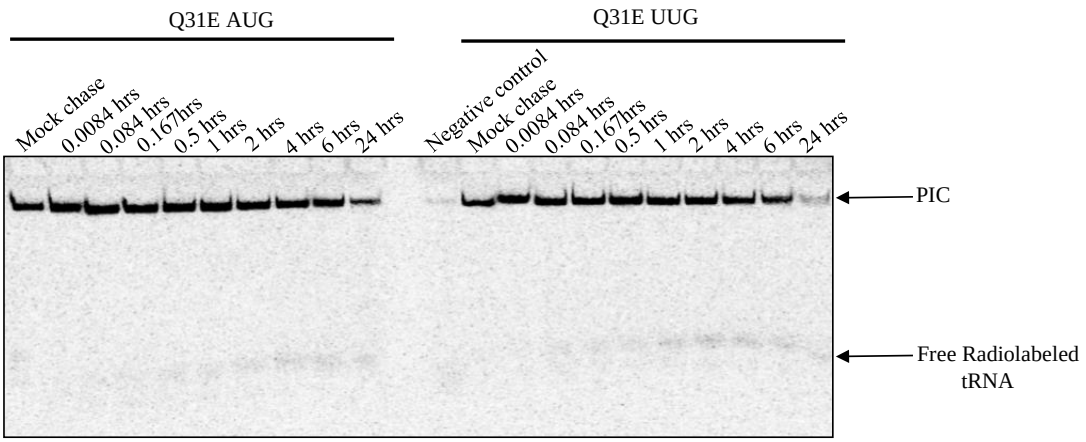
Q31E AUG
Q31E UUG
Mock chase
0.0084 hrs
0.084 hrs
0.167hrs
0.5 hrs
1 hrs
2 hrs
4 hrs
6 hrs
24 hrs
Negative control
Mock chase
0.0084 hrs
0.084 hrs
0.167hrs
0.5 hrs
1 hrs
2 hrs
4 hrs
6 hrs
24 hrs
PIC
Free Radiolabeled tRNA

Fig. S5. Representative results from TC dissociation assays. (A-C) To measure TC dissociation kinetics, as summarized schematically in (A), partial 48S complexes were assembled with radiolabeled TC, eIF1A, model mRNA containing an AUG or UUG start codon, and either WT eIF1 (B) or eIF1-Q31E (C). Following incubation at 26° C for two hours, each reaction was chased with excess unlabeled TC for increasing periods of time (between 0.0084 and 24 hours as indicated above gel image) and the fraction of labeled Met-$tRNA_i$ bound to the PIC at each time-point was determined by resolving radiolabeled 48S complexes (upper band) from free radiolabeled $tRNA_i$ (lower band) by EMSA. As a control, one reaction was chased with buffer only ('mock chase') for each eIF1/mRNA pair, representing the maximum possible PIC-bound radioactivity. One reaction was also conducted in which unlabeled chase was added before labeled TC ('negative control'), demonstrating the least possible PIC-bound radioactivity. The upper band from each lane was quantified and normalized to total radioactivity in the lane (after background subtraction). These values for each time point were normalized to the negative control and plotted as shown in Fig. 5H.

Fig. S6

A

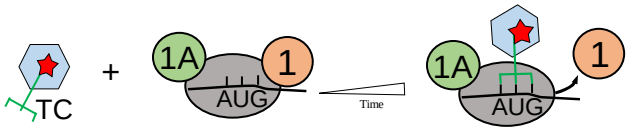
TC
+
1A
1
AUG
Time
1A
1
AUG

B

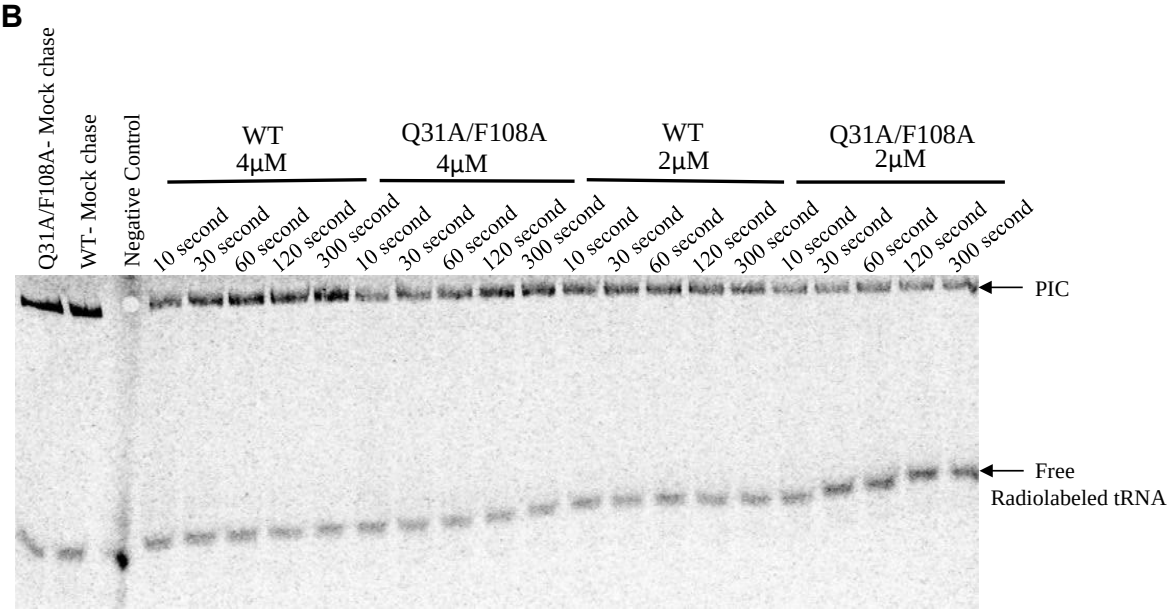
Q31A/F108A- Mock chase
WT- Mock chase
Negative Control
WT
4μM
Q31A/F108A
4μM
WT
2μM
Q31A/F108A
2μM
10 second
30 second
60 second
120 second
300 second
PIC
Free
Radiolabeled tRNA

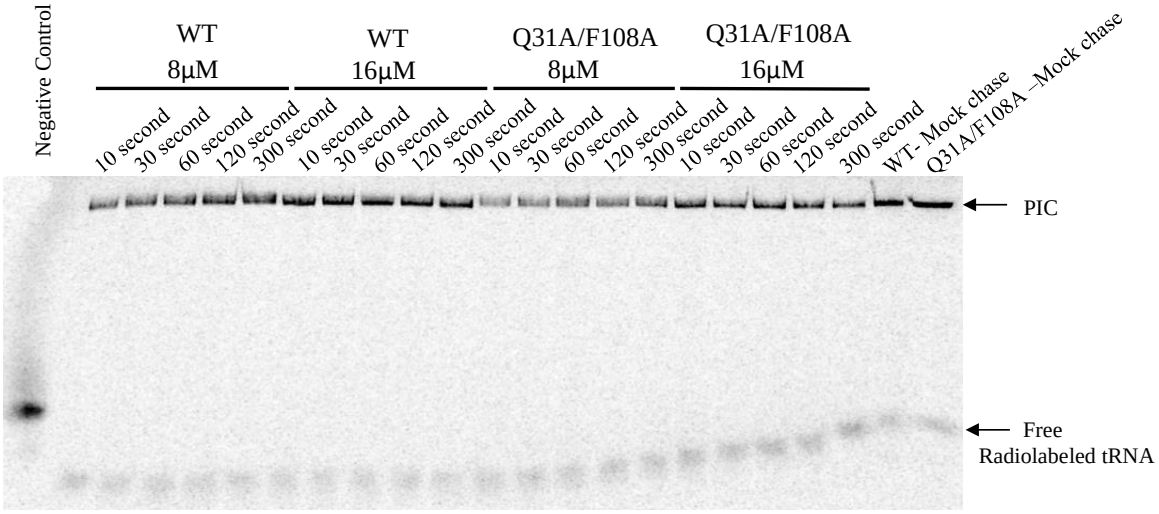
Negative Control
WT
8μM
WT
16μM
Q31A/F108A
8μM
Q31A/F108A
16μM
10 second
30 second
60 second
120 second
300 second
WT- Mock chase
Q31A/F108A –Mock chase
PIC
Free
Radiolabeled tRNA

Fig. S6. Representative results from TC association assays. (A, B) To measure TC association kinetics, as summarized schematically in (A), radiolabeled TC was mixed with pre-formed 40S·eIF1A·eIF1·mRNA complexes containing either WT eIF1 or eIF1-Q31A/F108A and incubated for increasing times (as indicated). Reactions for WT and mutant eIF1 were carried out at each of four concentrations of 40S ribosomal subunits (2 μM, 4 μM, 8 μM, and 16 μM, as shown). Reactions were terminated with a chase of excess unlabeled TC. The fraction of labeled Met-tRNA$_i$ bound to the PIC at each time-point was determined by EMSA, as in Fig. S5. As a control, one reaction was chased with buffer only ('mock chase'), representing the maximum possible PIC-bound radioactivity. One reaction was also carried out in which unlabeled chase was added before labeled TC ('negative control'), demonstrating the least possible PIC-bound radioactivity. For each time point, the upper band was quantified and normalized to total radioactivity in the lane (after background subtraction), followed by normalization to the negative control. These values were plotted to obtain the pseudo-first-order rate constant (k_{obs}) at each 40S concentration. The resulting k_{obs} values were plotted versus 40S concentration, as in Fig. 6B, to obtain the second-order rate constant (k_{on}).

Fig. S7

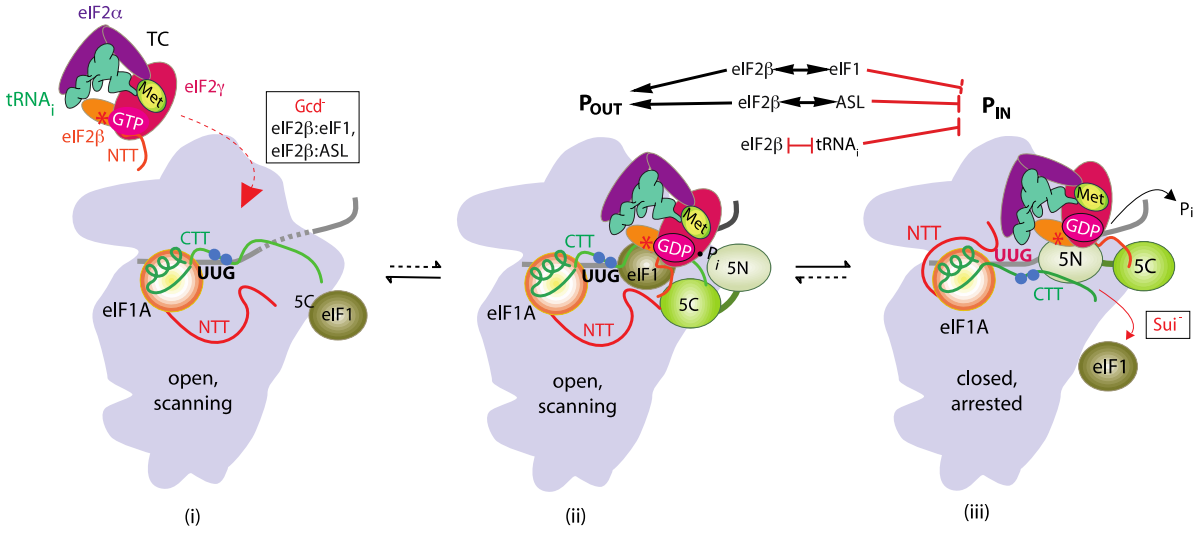

Fig. S7. Model describing the effects of eIF2β interactions on the conformational rearrangements of the PIC during start codon selection. As described in Fig. 1A, eIF1 and eIF1A promote an open, scanning conformation of the PIC to which TC loads (i). Mutations that destabilize the open conformation slow TC loading, resulting in a Gcd$^-$ phenotype. Following TC binding, the PIC scans the mRNA leader in the open conformation (ii). When a start codon is recognized, the PIC transitions to the closed state, accompanied by release of eIF1 and P_i (iii). Mutations that favor the closed complex, either by destabilizing the open state or by removing an impediment to transition to the closed state, decrease the fidelity of initiation, allowing selection of non-AUG codons including the near cognate UUG. Such mutations confer a Sui$^-$ phenotype. (Above) The arrows summarize the contributions of eIF2β to ensuring accurate start codon selection indicated by our findings here. The interactions of eIF2β with eIF1 and the ASL of $tRNA_i$ (Fig. S1D) stabilize and promote the open state, either by anchoring eIF1 to the complex or by stabilizing $tRNA_i$ binding, while impeding transition to the closed state. For this reason, substitutions at these interfaces confer both Gcd$^-$ and Sui$^-$ phenotypes. The clash of open-state eIF2β with the closed-state $tRNA_i$ D-loop (Fig. S1C), however, enforces a strict requirement for an AUG start codon and inhibits transition to the closed state in its absence, but does not stabilize the open state. Thus, substitutions at this interface produce Sui$^-$ phenotypes without any accompanying Gcd$^-$ phenotype.